



# Machine learning and economic forecasting: The role of international trade networks

Thiago Christiano Silva <sup>a,\*</sup>, Paulo Victor Berri Wilhelm <sup>a</sup>, Diego R. Amancio <sup>b,c</sup>

<sup>a</sup> Universidade Católica de Brasília, Distrito Federal, Brazil

<sup>b</sup> Department of Computing and Mathematics, Faculty of Philosophy, Sciences, and Literatures in Ribeirão Preto, Universidade de São Paulo, São Paulo, Brazil

<sup>c</sup> Institute of Mathematics and Computer Science, University of São Paulo, São Carlos, Brazil

## ARTICLE INFO

### Keywords:

International trade network  
Machine learning  
Economic forecast  
Economic growth  
De-globalization  
International trade  
Complex networks  
SHAP value

## ABSTRACT

This study examines the effects of de-globalization trends on international trade networks and their role in improving forecasts for economic growth. Using section-level trade data from more than 200 countries from 2010 to 2022, we identify significant shifts in the network topology driven by rising trade policy uncertainty. Our analysis highlights key global players through centrality rankings, with the United States, China, and Germany maintaining consistent dominance. Using a horse race of supervised regressors, we find that network topology descriptors evaluated from section-specific trade networks substantially enhance the quality of a country's economic growth forecast. We also find that non-linear models, such as Random Forest, eXtreme Gradient Boosting, and Light Gradient Boosting Machine, outperform traditional linear models used in the economics literature. Using SHapley Additive exPlanations values to interpret these non-linear models' predictions, we find that about half of the most important features originate from the network descriptors, underscoring their vital role in refining forecasts. Moreover, this study emphasizes the significance of recent economic performance, population growth, and the primary sector's influence in shaping economic growth predictions, offering novel insights into the intricacies of economic growth forecasting.

## 1. Introduction

In the evolving landscape of global economics, accurate forecasting of economic growth emerges as a cornerstone for crucial tasks, such as policymaking and investment decisions [1]. Traditional models for predicting GDP growth heavily rely on conventional economic indicators and standard linear econometric techniques [2]. However, the increasing complexity of global trade and economic interdependence calls for a more nuanced approach to forecasting. Recent advances in machine learning offer promising avenues for enhancing the performance and reliability of economic forecasts by processing large datasets and identifying complex, non-linear relationships [3]. This study contributes to two main strains of literature: analyzing international trade networks and applying machine learning models in economic forecasting. Specifically, it innovates by utilizing topological measures of international trade networks as features in machine learning models to forecast GDP growth and demonstrating that they substantially enhance the accuracy of GDP growth predictions for a country.

The significance of our work lies in its potential to provide a more comprehensive understanding of the factors driving economic growth predictions. This is particularly relevant in a world where economic landscapes are rapidly changing, and traditional

\* Correspondence to: Universidade Católica de Brasília, Câmpus I, QS 07 - Lote 01, EPCT, CEP: 71966-700, Taguatinga, DF, Brazil.

E-mail addresses: [thiagochris@gmail.com](mailto:thiagochris@gmail.com) (T.C. Silva), [paulo.wilhelm@gmail.com](mailto:paulo.wilhelm@gmail.com) (P.V.B. Wilhelm), [diegoraphael@gmail.com](mailto:diegoraphael@gmail.com) (D.R. Amancio).

forecasting models often fail to capture the dynamism of global interactions shaped by world trade. By integrating international trade network topologies into the machine learning framework, this study opens new pathways for research and offers practical insights for economists, policymakers, and investors seeking to navigate the complexities of the global market.

A substantial corpus of research leverages complex network theory to shed light on many topics in economics and finance.<sup>1</sup> The first part of our work deals with constructing trade networks and extracting topological measures. Multiple approaches to modeling the International Trade Network (ITN) are documented, such as binary and weighted configurations or directed and undirected networks [12,13]. Additionally, these models vary in terms of granularity, ranging from aggregated overviews to detailed breakdowns by very specific commodity types. Our research delves into the domain of commodity-specific trade networks, aligning with notable studies that explore various dimensions of the ITN through the lens of particular commodities.<sup>2</sup>

Our contribution to this literature has two principal dimensions. First, we explore commodity-specific trade networks through a section-level categorization delineated by the Harmonized System (HS) code framework. This approach enables us to extract topological characteristics that are particular to this granularity level, nuances frequently overlooked in current literature [22].<sup>3</sup> Secondly, we concentrate on the temporal evolution of the topological properties of the most significant commodity-specific networks from 2010 to 2022. This timeframe is especially pertinent for investigating trends of de-globalization, which have been intensified by critical global events such as the COVID-19 pandemic and the geopolitical tensions following Russia's invasion of Ukraine. Through this perspective, our analysis aims to elucidate the complexities of how commodity trade networks have adapted during these tumultuous periods, identifying which countries have either benefited from or been adversely affected by these changes.

In our analysis of the temporal dynamics of assortativity and network density, we observe a critical juncture between 2016 and 2018 that marks a reversal of previously noted trends, leading to significant topological transformations within the main section-level trade networks. This period coincides with a marked increase in trade policy uncertainty, underscoring the profound impact that trends towards de-globalization exerted during this timeframe.<sup>4</sup> Furthermore, we develop centrality rankings for the main commodity trade networks for the years 2010 and 2022, enabling the identification of key global actors and notable shifts in their influence over this period. Our findings affirm the United States' continued dominance as a leading player across four of the five principal commodity trade networks in 2022. Similarly, China and Germany have sustained high performance, consistently appearing in the top three to five rankings. This research documents various nations' ascension and decline in these rankings. Notably, Thailand's presence diminished significantly, falling from the top fifteen in 2010 to its absence in 2022 across the five main trade networks. In contrast, India showcases a remarkable trajectory, not featured in any of the top fifteen rankings in 2010, yet in 2022, it emerged in all five main trade networks, including three instances within the top five.

The second segment of our study engages with the literature that applies machine learning techniques to forecast economic growth. An expanding collection of research highlights that machine learning methods can surpass traditional econometric models in predicting GDP growth [24–27]. While these studies incorporate a diverse array of predictors, to our knowledge, they have yet to harness network topology metrics from international trade networks as predictive features.<sup>5</sup> We argue that integrating topological metrics into machine learning models can markedly enhance the precision of economic growth forecasts. Trade network-based descriptors are pivotal for two reasons. First, a country's trade network position reflects its global significance and product/service exchange flexibility. Second, today's economic trends in neighboring countries can indicate a nation's own economic prospects in the future. Thus, incorporating trade network measures enriches predictive models with a comprehensive view of global economic interactions.

Our study contributes by assessing the importance of network measures from commodity-specific trade networks on the performance of machine learning models for economic growth forecasting. A distinctive feature of the literature is that it generally focuses on one or a moderate number of countries. In this sense, we contribute by employing a “horse race” of machine learning models to identify the best-performing model in a disciplined way to forecast economic growth for a comprehensive set of more than 200 countries.<sup>6</sup> Accurate economic growth forecasts are essential to guide strategic decisions and global policy development.

<sup>1</sup> This body of work is extensive and includes analyses such as the behavior of stock returns amidst the Global Financial Crisis [4], the fluctuation patterns in stock prices [5], and the intricate relationship between the advent of COVID-19 and stock market dynamics [6]. Further exploration within this field includes the examination of the financial impacts stemming from shifts in monetary policy [7] and formulating investment strategies within a global framework [8]. The literature also navigates through the interconnectedness of global banking networks [9], the correlation between a firm's position in the supply chain structure and its innovation capabilities [10], and the evaluation of financial system vulnerabilities and the spread of economic impacts [11].

<sup>2</sup> These studies encompass a wide range of topics, including the evolutionary dynamics of the international fossil energy trade's multilayer network [14], the pivotal roles countries play within the international fossil fuel trade network [15], the spatiotemporal evolution of global plastic waste trade networks [16], and the community structure of the food-trade international multi-network [17]. Further contributions to the field examine the spatial-temporal evolution of the global copper raw materials and scrap trade networks [18], the characteristics and stability of the global complex nickel ore trade network [19], the analysis of wood and non-wood forest global trade network [20], the temporal stability of international fertilizer trade networks, and the multiplex network structure of global cobalt industry chain [21].

<sup>3</sup> Prevailing studies on international trade networks predominantly utilize aggregate trade data or examine it at a highly granular level. Adopting a section-level perspective for trade data affords us a compromise between these two extremes, which is crucial since the granularity of data can significantly influence topological characteristics.

<sup>4</sup> There was a notable trend towards globalization characterized by increasing openness to international trade. However, recent global events have contributed to heightened trade policy uncertainty and a shift towards protectionism and de-globalization [23].

<sup>5</sup> Several works utilize complex networks in forecasting tasks, including the use of stock networks to predict economic growth [28] and the predictability of stock price series through community detection and network metrics [29].

<sup>6</sup> Refers to a comparative evaluation among a variety of machine learning models to determine which performs best on a given task or dataset. This analogy draws from actual horse races, where horses compete to see which is fastest under similar conditions to identify the top performer.

By enabling policymakers to preempt economic instabilities, these forecasts contribute to a more stable economic climate. For businesses and investors, such insights are crucial for navigating market uncertainties and seizing growth opportunities. Additionally, in a closely interconnected global economy, the accuracy of these predictions is vital for international coordination in addressing economic challenges like trade imbalances and inflation. Thus, precise forecasts play a pivotal role in both national and global economic stability and collaboration.

In establishing a foundation for our analytical framework, we use the performance of the linear regression model as a baseline. This technique, notable for its simplicity in implementation and clarity in model interpretation, is a benchmark against which the efficacy of more advanced algorithms can be measured. By doing so, we can better measure the gains of using non-traditional methods. We introduce a suite of sophisticated, highly non-linear models into our study, including the Support Vector Machine, Light Gradient Boosting Machine, k-nearest neighbor, Random Forest, and XGBoost.

Given that these advanced non-linear methods have reduced model interpretability compared to linear regression, we employ the SHAP value analysis—a tool derived from the concept of Shapley value borrowed from game theory. This analytical tool enables us to restore a level of interpretability to these more complex and performant models. Through this approach, our contribution to the literature extends beyond merely identifying the superiority of non-linear machine learning methods compared to traditional linear regression. We provide a detailed exploration of how each feature contributes to the economic growth forecasts. We also provide economic rationale by elucidating the mechanisms through which they could affect economic growth. Consequently, our work enriches the literature with a comparative analysis of model performance and a deeper insight into the dynamics that drive economic growth predictions.

In our empirical evaluation, we consider four distinct error metrics to ascertain the average error values, thereby gauging the performance of models. Our findings delineate that the Random Forest, XGBoost, and k-NN models, in that order, emerge as the superior performers, with substantial enhancements over the baseline model. These outcomes suggest that the aforementioned models possess an inherent capacity to capture the complexities and non-linearities within the dataset, a task for which a linear regression model is inadequate.

We observe intriguing patterns when analyzing each feature's contribution to the overall prediction of the three best-performing models. Notably, the set of features with the greatest importance is consistent across all these models, underscoring their significance in economic growth forecasting. In particular, nearly half of the top fifteen most influential features for the Random Forest model — the most performing one — are network measures. This highlights the crucial role of commodity trade network topologies play in enhancing economic growth forecasts. Specifically, the density of the Mineral trade network emerges as a critical feature, ranking as the second most significant for both the Random Forest and XGBoost models, and as the foremost feature for the LightGBM model.

Additionally, our analysis brings to light the autoregressive nature of economic growth, where the immediacy and recency of GDP growth figures are pivotal in forecasting economic performance [30]. This observation lends credence to the concept of “economic inertia”, wherein past performance exerts a lingering influence on future outcomes. Moreover, we identify the significance of the modularity in the Machine & Electrical trade network, population growth, and relevance of the primary sector as key predictors of economic growth. These elements consistently feature among the top fifteen most relevant features across all three top-performing models, reinforcing their importance in the predictive models of economic performance.

To further elucidate interpretation insights, we conduct a comprehensive feature interpretability analysis on the most effective model, the Random Forest. In accomplishing this task, we utilize a suite of Shapley value dependence plots, which provide a detailed perspective on how fluctuations in feature values impact economic growth forecasts. One particularly intriguing pattern emerges when analyzing the density of the Mineral trade network. We observe that moderate escalations in this network measure are associated with neutral or beneficial effects on economic growth predictions. However, once a critical threshold is exceeded, further increases in network density are linked to a decline in future economic prospects. This discovery suggests an optimal range within which enhancements to network density can positively influence future economic growth, providing a critical insight into the nuanced interplay between trade network characteristics and economic forecasting.

Our research elucidates several policy implications. First, the significant topological transformations we document within global trade networks highlight their vulnerability to de-globalization trends. This observation necessitates a strategic reassessment by policymakers of economic policies heavily reliant on globalization mechanisms. Additionally, international collaboration must be fortified by a commitment to transparency in the formulation and implementation of policies. Such an approach is essential in mitigating uncertainty and cultivating a stable environment for international trade.

Furthermore, our analysis of centrality rankings unveils an evolving paradigm within the domain of international trade. This evolving landscape necessitates a proactive and forward-thinking approach to policy formulation. The sustained dominance of established economies, juxtaposed with the meteoric rise of emerging markets like India, signal dynamic shifts propelled by technological advancements and geopolitical developments.

Moreover, the outcomes of our comparative analysis of forecasting models reveal the intricate and non-linear nature of economic growth predictors. This complexity underscores policymakers' need to employ more sophisticated analytical frameworks in forecasting. Importantly, integrating network measures into forecasting models is as a powerful strategy to amplify the accuracy of economic growth predictions. Such enhanced predictive capability is invaluable, providing policymakers with the insights to craft more informed and efficacious policy measures.

2. Data and methodology

In this section, we present the data sources and methodologies employed in our study, which encompasses two distinct but complementary analyses. First, in Section 2.1, we outline the data and methods used to explore the fundamental properties of global trade networks through complex network analysis. This analysis examines the topological features and interconnections within commodity-specific trade networks, providing insights into the structural dynamics of global trade. Second, in Section 2.2, we detail the data and methodologies employed to forecast economic growth using machine learning techniques. This analysis leverages network metrics to predict future trends, aiming to enhance the accuracy and reliability of economic growth forecasts.

2.1. Complex network analysis of commodity-specific trade networks

Our research enhances the understanding of global trade by constructing networks derived from detailed trade data. Utilizing the Comtrade database<sup>7</sup> provided by the United Nations Statistics Division, we analyze bilateral merchandise trade information for 261 countries, dependent territories, and special areas of geographical interest.<sup>8</sup> This database organizes trade data according to the Harmonized System (HS) classification.<sup>9</sup> Our approach involves extracting data at the chapter level and then aggregating this information into section level, providing the most general categorization. To further reduce noise and ensure a clearer analysis, we transform the data's periodicity from monthly to quarterly during this aggregation process. Given the extensive nature of the official names for these sections, we use shortened names to improve both brevity and clarity in our presentation. Table 1 lists the code and associated abbreviated name for the ten most significant sections in terms of trade flow value from 2010 to 2022. The top five sections during this period accounted for approximately 60.7% of the global trade flow value.

Table 1  
The Top 10 most relevant commodity sections from 2010 to 2022.

Code	Abbreviated name	Relevance
16	Mechanical & Electrical	24.3%
5	Mineral	15.1%
17	Transport	10.5%
6	Chemical	10.0%
15	Base Metals	7.2%
7	Plastics & Rubber	4.6%
11	Textile	4.2%
14	Precious Metals	3.9%
18	Instruments	3.6%
4	Beverages & Tobacco	3.4%

Notes: In this table, Code corresponds to the identifier assigned to each commodity section according to the Harmonized System (HS) classification. Abbreviated name denotes the concise name we have devised to represent the official title of the section as defined by the HS classification. Relevance represents the section's trade value as a percentage of the total merchandise trade value from 2010 to 2022.

Transactions classified as re-importations and re-exportations are excluded to concentrate on standard trade activities. The Comtrade database records each trade occurrence from the perspectives of both participating entities (the importer and the exporter), thereby introducing a potential mismatch in the transacted volume between each pair of reporting entities. To mitigate the inconsistencies arising from this dual reporting, this study adopts a methodology where the data reported by the nation exhibiting a superior aggregate trade value within the network is prioritized. This approach is grounded in the hypothesis that data furnished by nations with larger trade values tend to be more accurate, particularly when trade involves nations with significantly disparate economic sizes.

In the commodity-specific trade networks we construct, we employ two directed graph representations: one weighted and the other unweighted. In both, nodes represent individual countries, while edges denote bilateral trade flows of a particular commodity section. Each edge is directed, originating from the exporting (or origin) country and terminating at the importing (or destination) country. For the directed weighted graph, edge weight signifies the monetary value of the respective bilateral trade flow. For the directed unweighted graph, edges indicate the presence of a trade relationship without considering the trade volume.

<sup>7</sup> <https://comtradeplus.un.org/>.

<sup>8</sup> We follow three-letter country codes defined in ISO 3166-1, part of the ISO 3166 standard published by the International Organization for Standardization (ISO).

<sup>9</sup> The Harmonized System of Tariff Nomenclatures, often referred to as the Harmonized System Classification, is a standardized system of names and numbers for classifying traded products. Developed and maintained by the World Customs Organization (WCO), the HS is utilized by over 200 economies as a basis for their customs tariffs and for collecting international trade statistics. The HS is designed to facilitate the international trade process by simplifying the identification and classification of goods across borders. The system is structured into 21 sections, further divided into 97 chapters. These chapters are subdivided into headings and subheadings, representing a hierarchical structure that classifies goods from the general to the specific. For more information, access: [HS Nomenclature 2022 edition](#).

We employ a set of graph representations that permit the calculation of different network metrics, providing unique topological representations of commodity trade networks. For our analytical purposes, we adopt a set of network metrics as delineated by Silva and Zhao [31], which encompass a diverse range of fundamental measures that encapsulate local, intermediate, and global network attributes (see Appendix A). This strategic selection enables us to elucidate the multifaceted topological characteristics of each section-level international trade network, ranging from the nuanced intricacies of individual trade connections to the overarching structure of global trade within the specific commodity category.

## 2.2. Economic growth forecasting with machine learning

### 2.2.1. Motivation

We use machine learning models to forecast country-specific Gross Domestic Product (GDP) growth. Our analysis builds upon traditional methods that predict GDP growth using country-specific variables by introducing network descriptors extracted from section-specific trade networks. We believe network-based descriptors can offer predictive power for two main reasons. Firstly, a country's position in the trade network may convey information on its importance to other peers and its ability to access and substitute products and services across its counterparts. Secondly, economic conditions in a country's neighbors may provide insights into its own economic variables. For instance, if a neighbor transacts less than historically with a specific country, this behavior may signal potential GDP growth challenges for that country in the upcoming years. Both features can potentially affect a country's GDP growth. Therefore, we include network measures to introduce a novel dimension to the analysis, shedding light on the impact of the topological properties of international trade networks on economic forecasting.

The pursuit of accurate economic growth forecasting is an endeavor that profoundly influences strategic decision-making and policy formulation across the globe. It equips policymakers with the tools to design proactive measures to smooth out economic fluctuations, fostering a more stable economic environment. For businesses and investors, the insights gleaned from these forecasts anchor expectations and provide foresight that helps navigate market uncertainties and leverage opportunities for growth and expansion. Moreover, the importance of these forecasts extends beyond national borders. In an interconnected global economy, the ripple effects of economic trends in one country can have far-reaching impacts. Accurate forecasts enable countries to synchronize their economic policies and responses, which is essential for managing global challenges such as trade deficits and inflationary pressures.

### 2.2.2. Data

We utilize machine learning methodologies to forecast economic growth, designating annual GDP growth as our target variable. This data is acquired from the World Bank's Open Data platform.<sup>10</sup> We incorporate two distinct sets of feature variables into our analysis to achieve our objective of predicting economic growth. We note that all data employed in this analysis refers to annual values. The initial set pertains to the fundamental characteristics of countries, which can further be categorized into relevant subsets. The sources of data for this analysis encompass the United Nations Conference on Trade and Development<sup>11</sup> and the World Bank's Open Data platform:

- Main economic indicators: GDP per capita (PPP); GDP (US\$); GDP growth;  $GDP_{t-1}$  growth;  $GDP_{t-2}$  growth; GDP deflator (%); Gross capital formation to the labor force; Unemployment rate (%); Labor force participation rate (%); Agriculture, forestry, and fishing (% of GDP); Manufacturing (% of GDP); Services (% of GDP); Carbon dioxide emissions per capita (tonnes); and Material footprint per capita (tonnes).
- Economic openness: stimulates growth by fostering competition and efficiency, leading to technological advancements and productivity gains. It expands access to global markets, enhancing export opportunities and enabling firms to achieve economies of scale. Furthermore, it attracts foreign investment and facilitates knowledge transfer, contributing significantly to a country's economic development [32]. We select the following variables: Trade (% of GDP); Net trade in goods (US\$); Current account balance (% of GDP); PPP conversion factor; Net inflows of foreign direct investment (% of GDP); and Inward foreign direct investment stock.
- Institutional quality: Governmental institutions lay the foundation for a country's economic activities. Effective institutions foster an environment conducive to economic engagement, innovation, growth, and development [33]. We employ measures of Regulatory quality, Rule of law, Government effectiveness, Control of corruption, and Voice and Accountability.
- Infrastructure: is a critical determinant of economic growth, acting as a catalyst for improving efficiency, productivity, and connectivity [34]. To account for the infrastructure quality, we employ: Fixed broadband subscriptions (per 100 people); Access to basic sanitation (% population); and Urban population (% population).
- Human development: Education significantly boosts economic growth by enhancing workforce productivity and fostering innovation, which leads to increased efficiency and groundbreaking advancements [35]. Health is a crucial driver of economic growth, primarily by enhancing labor productivity and reducing healthcare costs, thereby increasing economic efficiency and output [36]. We employ the following measures: Mean years of schooling, Human development index, Human inequality, Life expectancy at birth, Refugee population, and Population growth (%).

<sup>10</sup> <https://data.worldbank.org/>.

<sup>11</sup> <https://unctadstat.unctad.org/EN/>.



Our second set of feature variables consists of network measures derived from section-level international trade networks developed during the network analysis phase. We average the quarterly values for network metrics extracted from these networks to obtain annual measures, thus eliminating the need to construct new trade networks. These annual network metrics align with the corresponding annual economic and social indicators. We consider all network metrics across the most relevant sections: Mechanical & Electrical, Mineral, Transport, Chemical, and Base Metals.

In our research, we execute several pre-processing steps on our dataset before applying machine learning models to ensure the integrity and quality of our analysis. Initially, we transform all nominal predictor variables into factor variables. Further refining our dataset, we filter out features exhibiting a correlation higher than 0.9 to mitigate the effects of multicollinearity, ensuring that highly correlated predictors do not skew our model's performance. Additionally, we eliminate features with near-zero variance, specifically those with a dominant category not sufficiently balanced by other categories, as identified by a frequency cut-off of 100.<sup>12</sup> This step is essential for removing variables unlikely to contribute significantly to the model's predictive accuracy.

We employ the k-NN imputation method to address missing values, leveraging the algorithm to estimate and replace missing data with the most plausible values based on similar observations. We also normalize all numeric predictors, excluding the "year" variable, to prevent variables with larger scales from overpowering those with smaller scales, ensuring each contributes equally to the model's efficacy. In the subsequent stage of our data preparation, we convert nominal predictors previously transformed into multiple dummy (binary) variables, each representing a category of the nominal predictor.

After executing our pre-processing steps, our data matrix has dimensions of 3062 rows by 99 columns. This matrix represents an unbalanced panel comprising 60 network metrics and 39 economic variables for each layer.

### 2.2.3. Horse race of machine learning models

We use a horse race to select among a set of supervised learning regression techniques. The suite of machine learning models applied includes the Light Gradient Boosting Machine (LightGBM), Support Vector Machines (SVM), k-nearest neighbor (k-NN) algorithms, Extreme Gradient Boosting (XGBoost), Linear Regression and its regularized variants, and Random Forest (see [Appendix B](#)). This diverse array of models facilitates a thorough analysis by capturing the complex, both linear and non-linear, relationships between country-specific factors and the structure of section-level trade networks. We use variables in  $t$  to predict  $y_{t+1}$ , where  $y_{t+1}$  represents economic growth in  $t+1$ . We use the same training and prediction sets for all the machine learning algorithms to ensure a fair comparison.

In our model selection procedure, we use a cross-validation technique to search for each algorithm's most effective combination of hyperparameters, thereby optimizing predictive performance and ensuring model generalization to unseen examples. Hyperparameters, which are external configurations to the model that cannot be learned from the data, influence the training process and the architecture of the machine learning model. We undertake the hyperparameter tuning process by systematically navigating a predefined grid of hyperparameter values and evaluating model performance through adaptive resampling via futility analysis [37].<sup>13</sup> We set the Root Mean Squared Error (RMSE) as our performance metric in the model selection. The model (and corresponding optimal set of hyperparameters) that minimizes the average RMSE across all models in the cross-validation procedure will be the winner in the horse race.

We evaluate the contributory significance of each feature within our predictive models by employing SHAP (SHapley Additive exPlanations) values [38]. Shapley values, originating from game theory literature, provide a systematic approach to fairly distribute the total gains among participants based on their individual contributions [39]. This concept has been adapted to machine learning to evaluate the interpretability and importance of features within predictive models. By examining all possible permutations of features, Shapley values ensure a fair allocation of contributions based on the marginal impact of each feature.

$$\phi_i(v) = \sum_{S \subseteq N \setminus \{i\}} \frac{|S|!(n - |S| - 1)!}{n!} (v(S \cup \{i\}) - v(S)) \quad (1)$$

where  $\phi_i(v)$  represents the Shapley value for feature  $i$ ,  $N$  is the set of all features,  $n$  is the total number of features,  $S$  is a subset of features excluding  $i$ , and  $v(S)$  is the prediction function for subset  $S$ . This equation encapsulates the essence of Shapley values by quantifying the marginal contribution of feature  $i$  when added to a subset of features  $S$ .

However, computing Shapley values directly for complex models can be computationally intensive due to the factorial growth of possible feature combinations. This is where SHAP values come into play. SHAP values are an approximation of Shapley values, designed to mitigate computational hurdles while retaining the interpretability and fairness properties of Shapley values. By leveraging efficient algorithms and approximations, SHAP values make the assessment of feature importance feasible in real-world machine learning applications.<sup>14</sup> The principle of marginal contribution, pivotal to SHAP values, evaluates the additional impact of

<sup>12</sup> A frequency cut-off of 100 refers to the ratio of the frequency of the most common value to the frequency of the second most common value in a predictor. Specifically, a predictor is considered to have near-zero variance if the most frequent value appears at least 100 times more often than the second most frequent value. This stringent threshold ensures that only the most unbalanced predictors, which provide minimal discriminatory power and could lead to overfitting, are removed from the dataset. This helps improve model performance, reduce overfitting, and simplify the model.

<sup>13</sup> Futility analysis enhances efficiency by quickly discarding poorly performing hyper-parameter configurations. It involves initial performance evaluation on a small data subset or limited cross-validation and early elimination of underperforming configurations. This approach focuses resources on promising configurations, reducing the total number of evaluations. Consequently, computational time is decreased, speeding up the tuning process and ensuring the final model uses the most effective parameters for optimal performance.

<sup>14</sup> We use the `fastshap` package in RStudio to calculate SHAP values. This package employs Monte Carlo algorithms for approximation, using sampling and heuristic methods to make the computation feasible [40].

including a specific feature in a subset of features on the predictive outcome. SHAP values are calculated for each feature across all possible combinations, yielding a detailed portrayal of feature importance that is model-agnostic. This enables the interpretation of complex models by revealing the impact of each feature on the prediction for each instance in the dataset.<sup>15</sup>

### 3. Results and discussion

In this section, we present and analyze the findings from our study. First, in Section 3.1, we delve into the topological changes in commodity trade networks, indicating emerging patterns of deglobalization. We analyze the temporal dynamics of fundamental network metrics and reveal significant shifts in network centrality during recent periods, highlighting changes in influence within the main international trade markets. Next, in Section 3.2, we explore the potential of section-level trade network measures as predictors for GDP growth through a machine learning approach. We conduct a comparative analysis to rank machine learning algorithms based on their forecast performance. Additionally, we examine feature importance and interpretability for the top-performing models using SHAP values.

#### 3.1. Topological changes in commodity trade networks and emerging deglobalization patterns

In this subsection, we provide a topological examination of section-level international trade networks, focusing on the period from 2010 to 2022. This interval is convenient for understanding the dynamics of globalization, as it marks the emergence of signs pointing to a deglobalization process. During this period, several pivotal events profoundly impacted global trade dynamics, including Brexit, the China–USA trade war, the COVID-19 pandemic, and Russia's invasion of Ukraine. Given the expansive scope of this analysis, our investigation is streamlined to concentrate on the five most significant commodity sections of this period. Collectively, these sections account for approximately 60% of the monetary trade value within the specified timeframe, thereby providing a comprehensive overview of the critical trends and shifts in international trade patterns during a period marked by considerable geopolitical and economic upheavals. The network topological analysis uses a quarterly aggregation period, allowing for a detailed and granular understanding of the evolving trade relationships and network structures.

First, we explore topological dynamics by examining the temporal evolution of five key network measures. These metrics provide a detailed view of the changing structural properties of the networks, highlighting shifts in trade relationships and the emergence of new patterns over time. Next, we analyze the centrality dynamics within these networks, focusing on the centrality rankings of countries in 2010 and 2022. This comparison reveals significant shifts in countries' positions within the trade networks, underscoring the changing landscape of global trade.

##### 3.1.1. Topological dynamics in leading commodity trade networks

Fig. 1 depicts the evolution of five fundamental network measures for the most traded commodity sections from 2010 to 2022. Initially, we examine the network density measure. Among the sections analyzed, Mechanical & Electrical exhibits the highest average network density value of 0.314, indicating that, on average, 31.4% of the potential trade connections between countries are realized within this section. Conversely, the Mineral section presents the lowest average density value, 0.179, which corresponds to merely 57% of the value observed for the Mechanical & Electrical section. The average density values for the remaining sections are as follows: Chemical (0.261), Base Metals (0.256), and Transport (0.219). A noteworthy observation is the bifurcation in trends during the analyzed period; from 2010 to 2017, an increase in density values suggests enhanced interconnectedness among trading partners. However, post-2017, a trend toward stagnation or decline is observed. Notably, the Mechanical & Electrical section demonstrates stability in its density value throughout the period, whereas the Base Metals, Transport, and Mineral sections exhibit a clear downward trajectory. The onset of the COVID-19 pandemic in early 2020 prompted a sharp decline in the density values of the Transport and Chemical sections, while the Mechanical & Electrical section experienced a less pronounced impact, highlighting the heterogeneous effects of the pandemic on trade network interconnectedness.

Turning our attention to the assortativity network measure, all sections reveal predominantly negative assortativity values, suggesting prevalent trade interactions between heterogeneous countries (i.e., nations with a disparate number of partners). The Mechanical & Electrical section stands out with the most negative average value of  $-0.432$ , while the Mineral section records the least negative average assortativity value of  $-0.343$ . The assortativity values for the other sections are as follows: Base Metals ( $-0.405$ ), Transport ( $-0.379$ ), and Chemical ( $-0.369$ ). Temporal analysis of these values reveals two distinct phases. Until mid-2014, a shift towards less negative assortativity values indicates a trend towards more homogeneous commercial relationships. Contrarily, after 2017, this trend reversed, with assortativity values becoming more negative, culminating in 2022 with lower values than those recorded in 2010 for all sections, excluding Mechanical & Electrical. This recent trend underscores the disassortative nature of these trade networks.

The analysis of the temporal evolution of assortativity and network density suggests that a pivotal shift occurred during 2016–2018, reversing earlier observed trends and inducing profound topological alterations within the main section-level trade networks. This period aligns with a significant surge in the Trade Policy Uncertainty Index [23].<sup>16</sup> Such dramatic rises in trade

<sup>15</sup> Some interesting applications of SHAP values in machine learning models include identifying mortality factors during the COVID-19 pandemic [41], estimating the state of Li-ion batteries [42], and predicting bitcoin prices [43].

<sup>16</sup> Originating in 1960, this index experienced its most pronounced increase during this timeframe. Specifically, the index's monthly average escalated from 27.3 (2010–2015) to 114.3 (2016–2019), with peaks exceeding 200 in certain months.

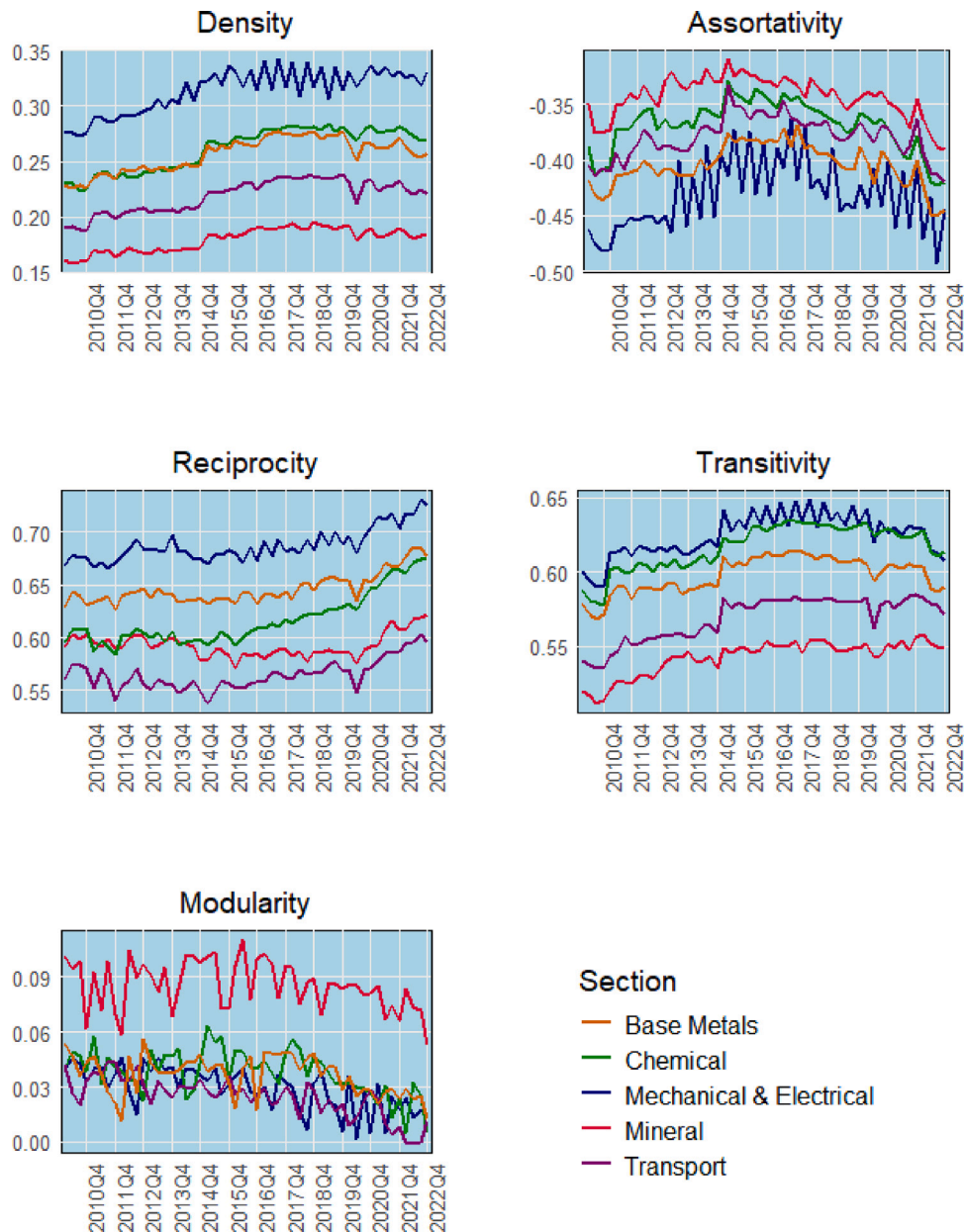


**Fig. 1.** This figure presents an analytical overview through five distinct plots, illustrating the evolution of key topological metrics within international trade networks from 2010 to 2022. Each plot tracks the temporal progression of a particular network measure for each of the five main section-level trade networks under scrutiny. The analysis employs a quarterly temporal resolution.

uncertainty underscore the detrimental impacts of critical geopolitical and economic events on global trade within the last decade. This correlation between the surge in trade policy uncertainty and our findings suggests that heightened trade policy uncertainty correlated with lower network connectivity and prompted more peripheral countries to re-establish connections with central trade hubs. The economic rationale behind this observed trend is attributed to an increased risk aversion amid rising economic uncertainty. In the period preceding 2016–2018, characterized by relatively low trade policy uncertainty, countries were more inclined to engage in international trade, actively seeking new partnerships, often with peripheral nations within the trade network. This era witnessed an increase in assortativity, with peripheral countries predominantly engaging in transactions with similarly positioned entities, i.e., other peripheral countries.

However, the landscape shifted dramatically after 2018 amidst the mounting trade uncertainty and heightened risk aversion. Trade patterns began to coalesce around more established, central countries within the network, denoting a strategic pivot in economic interactions. Peripheral nations, in response, scaled back their trade transactions with similarly peripheral counterparts,



opting instead to prioritize transactions with more central entities, perceived as safer counterparts. This strategic realignment precipitated a decline in assortativity, marking a transformative phase in the connectivity patterns of the main section-level trade network.

Continuing our topological examination, we delve into the dynamics of reciprocity and clustering patterns across the primary commodity trade networks. Regarding reciprocity, all sections consistently exhibit average values above 0.500 throughout the analysis period, underscoring a prevalent trend of reciprocal trade relations among countries. The Mechanical & Electrical section stands out with the highest average reciprocity, achieving 0.688, while the Transport section presents the lowest, at 0.565. The average reciprocity for the remaining sections is as follows: Base Metals (0.646), Chemical (0.617), and Mineral (0.592). A temporal analysis reveals distinct trends: the Mechanical & Electrical section shows a unique and consistent increase in reciprocity throughout the period. The Base Metals and Chemical sections display relatively stable values up to 2015, followed by a noticeable rise. The Mineral and Transport sections initially exhibit a decline, yet from 2016, Transport experienced a resurgence in reciprocity, with Mineral showing recovery only from 2020 onwards. Interestingly, the Chemical and Mineral sections, which had similar reciprocity levels in 2010, diverged post-2014, with the Chemical's increased reciprocity aligning it more closely with Base Metals. By the end of the analysis period, all sections show a trend towards higher reciprocity, indicating a strengthening of reciprocal trade relations over time.

Concerning local clustering behavior, we note that each section maintains an average transitivity value above 0.540, indicating significant local clustering. The Mechanical & Electrical section has the highest average transitivity at 0.624, with Mineral recording the lowest at 0.543. The figures for the other sections are Chemical (0.616), Base Metals (0.600), and Transport (0.569). Temporal dynamics of this metric unveil varying patterns: all sections witness an increase in local clustering up to mid-2014. From 2014 to 2019, transitivity stabilizes, halting the previous upward trend. The onset of the COVID-19 pandemic leads to a notable drop in clustering, especially within the Transport and Mechanical & Electrical sections. After 2019, a general decline in clustering was observed, except for the Mineral section, which showed resilience by maintaining its pre-pandemic transitivity values. Additionally, the period under analysis sees the Chemical section's transitivity converging with that of the Mechanical & Electrical, with the first ultimately exhibiting the highest transitivity by 2022.

We assess modularity patterns to conclude the first part of our topological analysis. Across all sections, average modularity values remain exceedingly low, approaching zero, throughout the studied period. Considering the significant local clustering identified earlier, these minimal modularity values highlight a key aspect of the networks' structure. Despite a tendency for countries' trade partners to form interconnected clusters, these section-level trade networks lack a modular organization, suggesting the absence of distinct segregation in trade interactions among specific groups. This finding suggests the existence of many countries serving as bridges connecting peripheral countries.

### 3.1.2. Centrality dynamics in leading commodity trade networks

Centrality, measured by PageRank and representing the influence of countries in commodity trade markets under the perspective of import performance, is the focus of the second part of our topological analysis, which looks into shifts in ranking centrality between 2010 and 2022. Table 2 reports centrality rankings for the following sections: Mechanical & Electrical and Chemical. Regarding the Mechanical & Electrical section, the United States is the most central country for both years under review. Following closely, China and Germany constitute the Top 3, with Germany ascending to the second position by 2022. We highlight the fall in the rank position of the following three countries: Great Britain descends from the fifth to the tenth position, Singapore from the ninth to the twelfth, and Japan from the twelfth to the fifteenth. Conversely, Mexico exhibits an upward trajectory, advancing from the seventh to the fourth position. Additionally, entry and exit dynamics from the Top 15 list reveal notable shifts. Thailand, previously ranked fourth in 2010, vanishes from the 2022 ranking. Similarly, Russia, Malaysia, and Spain, present in the 2010 rankings, are absent in 2022. Four nations — Hong Kong, India, the Republic of Korea, and the United Arab Emirates — were not listed in 2010 and appeared in the 2022 ranking. Among these, Hong Kong and India are particularly prominent, securing the seventh and ninth positions, respectively.

In examining the Chemical section, the United States emerges as the most dominant entity, with China and Germany trailing closely behind. This analysis reveals a growing influence of the United States and China over the observed period, as indicated by the relative decline in the centrality metrics of other nations. Particularly noteworthy is the ascension through the ranks of the Netherlands, Belgium, Canada, Brazil, India, and the Republic of Korea, with India's rise to the fourth position by 2022 being especially remarkable. On the contrary, there is a noticeable descent in the standings of France, Great Britain, Japan, Italy, and Spain. Despite these shifts, the overall makeup of the Top 15 has shown remarkable consistency, except for Thailand's departure, which paved the way for Mexico's entry.

Table 3 reports centrality rankings for the following sections: Mineral and Transport. The findings for the Mineral section underscore China's ascendancy as the preeminent nation within this network. Notably, the United States retained its second-place standing; however, its proximity to China's centrality value in 2010 — amounting to 80% of the leader's score — dwindled by 2022, falling to 45%. This significant reduction accentuates the solidification of China's network influence. We draw attention to the upward trajectory of Australia, the Republic of Korea, France, and the Netherlands in the 2022 rankings. The Republic of Korea, in particular, merits acknowledgment for its climb from the eleventh to the seventh position, indicating a notable increase in its centrality within the network. Conversely, the ranking declined for Belgium, Hong Kong, Italy, Japan, and Singapore. Specifically, Hong Kong's descent from the eighth to the fourteenth position and Belgium's fall from the tenth to the fifteenth position are highlighted as significant shifts. Regarding ranking composition changes, we point out the exit of only two countries, Thailand and

**Table 2**

In this table, we present the Top 15 centrality rankings for the following sections: Mechanical & Electrical and Chemical. The rankings are delineated in two separate panels, with the left panel showcasing the data for 2010 and the right panel for 2022.

2010			2022		
Rank	Centrality	Country	Rank	Centrality	Country
<b>Mechanical &amp; Electrical</b>					
1	100%	United States	1	100%	United States
2	57%	China	2	46%	Germany
3	53%	Germany	3	45%	China
4	50%	Thailand	4	30%	Mexico
5	37%	Great Britain	5	25%	France
6	33%	France	6	25%	Canada
7	30%	Mexico	7	24%	Hong Kong
8	28%	Netherlands	8	22%	Netherlands
9	27%	Singapore	9	21%	India
10	26%	Canada	10	20%	Great Britain
11	21%	Italy	11	16%	Italy
12	21%	Japan	12	14%	Singapore
13	19%	Russia	13	14%	Republic of Korea
14	17%	Malaysia	14	13%	United Arab Emirates
15	15%	Spain	15	13%	Japan
<b>Chemical</b>					
1	100%	United States	1	100%	United States
2	64%	China	2	65%	China
3	59%	Germany	3	53%	Germany
4	43%	France	4	31%	India
5	35%	Thailand	5	30%	France
6	33%	Great Britain	6	30%	Netherlands
7	32%	Japan	7	27%	Brazil
8	32%	Netherlands	8	25%	Belgium
9	31%	Belgium	9	25%	Canada
10	27%	Canada	10	24%	Great Britain
11	25%	Italy	11	24%	Japan
12	24%	Spain	12	20%	Italy
13	23%	Brazil	13	19%	Republic of Korea
14	20%	India	14	18%	Spain
15	19%	Republic of Korea	15	17%	Mexico

Notes: In our analysis, we have normalized the centrality values to facilitate a comparative understanding of each country's relative centrality within the specific section-level trade network. This normalization process adjusts the centrality scores, ensuring they are expressed in relation to the most central nation within each respective network.

Canada, which were positioned towards the lower end of the Top 15 in 2010. The entry of India and Malaysia into the rankings is noteworthy, particularly India's impressive positioning at fourth place in 2022.

In Transport, Thailand's prominent role in 2010 diminished completely by 2022. The United States, ascending from second place in 2010, secured the leading position by 2022. This advancement positions the United States at the pinnacle of the section, followed closely by Germany and France, who climb to the second and third positions, respectively, thereby delineating the top echelon in 2022. Great Britain, Canada, and China improved their positioning in 2022, with China showing the most substantial climb from the eleventh to the sixth position, highlighting its growing influence in the Transport section. Conversely, Australia and Spain experienced a decline, with Australia dropping from the fifth to the fifteenth position. Composition shifts in the Top 15 of the Transport section is marked by the exit of five countries: Thailand, Russia, Saudi Arabia, Japan, Indonesia, and Brazil, introducing new participants such as Belgium, the United Arab Emirates, Poland, Mexico, and the Netherlands, thus reflecting the evolving landscape of this network.

We report centrality rankings for the Base Metals section in Table 4. The United States maintains and amplifies its leadership, underlining a consolidation of influence as centrality values for the remainder of the Top 15 experience a noticeable decline in 2022. China and Germany remain steadfast, mirroring the top-tier dynamics observed in the Mechanical & Electrical and Chemical sections. The trajectory for five countries — Italy, France, Japan, Great Britain, and the Netherlands — points downwards. However, Japan presents an anomaly, shifting from sixth place in 2010 to fifth in 2022, indicating a nuanced change in its network centrality. Conversely, Canada, Turkey, Mexico, and the Republic of Korea ascend within the rankings, with Mexico's commendable leap from twelfth to fourth position emphasizing its enhanced role in the network. The period under review witnesses the departure of Thailand and Belgium from the rankings, making room for India and Poland's entry. India, in particular, garners attention by securing the fifth position, showcasing its significant ascendancy within the Base Metals sector.

### 3.2. Trade network measures as predictors: a machine learning approach to GDP growth forecasting

In this subsection, we present the results of our machine learning approach to economic growth forecasting, utilizing trade network measures as predictors to enhance forecasting performance. First, we evaluate the predictive accuracy of various supervised

**Table 3**

In this table, we present the Top 15 centrality rankings for the following sections: Mineral and Transport. The rankings are delineated in two separate panels, with the left panel showcasing the data for 2010 and the right panel for 2022.

2010			2022		
Rank	Centrality	Country	Rank	Centrality	Country
<b>Mineral</b>					
1	100%	China	1	100%	China
2	80%	United States	2	45%	United States
3	53%	Singapore	3	40%	Netherlands
4	50%	Japan	4	37%	India
5	37%	Germany	5	37%	Germany
6	35%	Netherlands	6	34%	Singapore
7	29%	Italy	7	34%	Republic of Korea
8	28%	Hong Kong	8	33%	France
9	27%	France	9	33%	Japan
10	22%	Belgium	10	31%	Italy
11	22%	Republic of Korea	11	25%	Australia
12	22%	Australia	12	21%	Malaysia
13	22%	Spain	13	19%	Spain
14	21%	Thailand	14	18%	Hong Kong
15	21%	Canada	15	18%	Belgium
<b>Transport</b>					
1	100%	Thailand	1	100%	United States
2	48%	United States	2	64%	Germany
3	46%	Germany	3	39%	France
4	31%	France	4	32%	Great Britain
5	25%	Australia	5	32%	Canada
6	24%	Great Britain	6	24%	China
7	17%	Canada	7	24%	India
8	17%	Spain	8	23%	Netherlands
9	16%	Italy	9	20%	Italy
10	15%	Russia	10	20%	Mexico
11	15%	China	11	18%	Spain
12	14%	Saudi Arabia	12	17%	Poland
13	13%	Japan	13	17%	United Arab Emirates
14	13%	Indonesia	14	16%	Belgium
15	12%	Brazil	15	15%	Australia

Notes: In our analysis, we have normalized the centrality values to facilitate a comparative understanding of each country's relative centrality within the specific section-level trade network. This normalization process adjusts the centrality scores, ensuring they are expressed in relation to the most central nation within each respective network.

**Table 4**

This table presents the Top 15 centrality rankings for the Base Metals section. The rankings are delineated in two separate panels, with the left panel showcasing the data for 2010 and the right panel for 2022.

2010			2022		
Rank	Centrality	Country	Rank	Centrality	Country
<b>Base Metals</b>					
1	100%	United States	1	100%	United States
2	85%	China	2	57%	Germany
3	75%	Germany	3	55%	China
4	42%	Italy	4	34%	Mexico
5	39%	France	5	32%	India
6	37%	Japan	6	32%	Canada
7	37%	Canada	7	31%	Italy
8	32%	Netherlands	8	26%	France
9	32%	Thailand	9	22%	Turkey
10	31%	Great Britain	10	22%	Republic of Korea
11	29%	Turkey	11	20%	Netherlands
12	28%	Mexico	12	20%	Great Britain
13	28%	Republic of Korea	13	18%	Poland
14	26%	Spain	14	17%	Spain
15	23%	Belgium	15	17%	Japan

Notes: In our analysis, we have normalized the centrality values to facilitate a comparative understanding of each country's relative centrality within the specific section-level trade network. This normalization process adjusts the centrality scores, ensuring they are expressed in relation to the most central nation within each respective network.

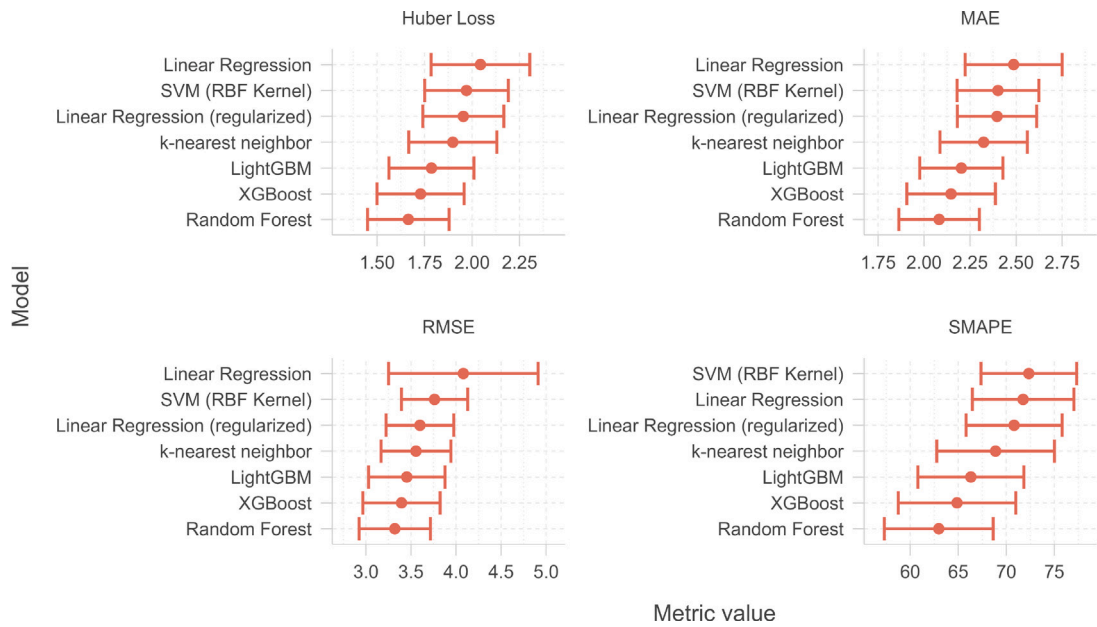


**Fig. 2.** This figure illustrates the estimated error values and their associated confidence intervals for the four error metrics — Huber Loss, Mean Absolute Error (MAE), Root Mean Square Error (RMSE), and Symmetric Mean Absolute Percentage Error (SMAPE) — evaluated across the seven machine learning algorithms examined in our study.

machine learning algorithms employed in our horse race procedure by using a set of performance metrics to rank the best models. Next, we analyze the importance of each feature's contribution to the economic growth forecast using SHAP value analysis for the three best-performing models. Lastly, we conduct a deeper analysis of feature importance and interpretability by examining beeswarm and dependence plots constructed with SHAP values for the top-performing model in our horse race.

### 3.2.1. Predictive accuracy

We use the RMSE as the criterion to select the best model. However, we also report other metrics to show that the selected algorithm is robust when we compare other performance metrics: Huber Loss, Mean Absolute Error (MAE), Root Mean Square Error (RMSE), and Symmetric Mean Absolute Percentage Error (SMAPE).<sup>17</sup> Achieving lower values across these metrics signifies superior predictive accuracy, indicating that the model's forecasts are consistently closer to the actual observed values.

In Fig. 2, we detail the average error values and their corresponding 95% confidence intervals across the four error metrics evaluated for the seven machine learning models included in our study over each of the out-of-sample remaining fold in the cross-validation procedure. The analysis elucidates a clear hierarchical structure in model performance, with the Random Forest model leading and closely followed by XGBoost and LightGBM.<sup>18</sup> Subsequent positions are occupied by k-NN, regularized Linear Regression, SVM with RBF Kernel, and, finally, Linear Regression. Generally, this ranking is maintained across the performance metrics.

### 3.2.2. Individual feature contribution to the economic growth forecast

Through SHAP value analysis, we aim to extract feature importance and interpretability from the three best-performing models. Fig. 3 displays the average SHAP values in the module for the Top 15 most influential features as identified across the three highest-performing models in our analysis. Notably, current GDP growth emerges as the paramount feature in both the Random Forest and XGBoost models, whereas it ranks second in the LightGBM model. A particularly striking observation is the pronounced dominance of this feature in the Random Forest model, where its SHAP value is approximately twice as large as that of the second-ranking

<sup>17</sup> The Huber Loss merges squared loss for small deviations and absolute loss for larger ones, effectively managing outliers with less severe penalties. This trait benefits economic data prone to outliers from economic shocks or errors. MAE calculates the average error magnitude, offering straightforward interpretability without weighing the direction of errors. Its limitation is the equal treatment of all errors, potentially overlooking significant prediction mistakes. RMSE amplifies larger errors by squaring them, enhancing sensitivity to outliers, and spotlighting models with occasional inaccurate predictions, but this also means RMSE is less tolerant of outliers than MAE. SMAPE uses percentage errors, ensuring scale independence and suitability for comparing different datasets, although its reliability falters with values near zero, restricting its use in certain cases.

<sup>18</sup> The optimal hyperparameter configurations for our suite of machine learning models are as follows: For the Elastic Net model, the optimal penalty is 0.007739036873, and the mixture parameter is 0.6662955002. For the SVM (RBF kernel), the cost is 0.5971530254, and the RBF sigma is 0.003403106644. The k-NN model requires 11 neighbors, utilizing an inverse distance weighting function and a distance power of 0.9160159697. The Random Forest model has an mtry value of 39 — indicating the number of features considered for splitting at each tree node — alongside a minimum node size of 12. For XGBoost, there are 861 trees and a learning rate of 0.01860805586, whereas the LightGBM model requires 1107 trees and a learning rate of 0.03441793697.

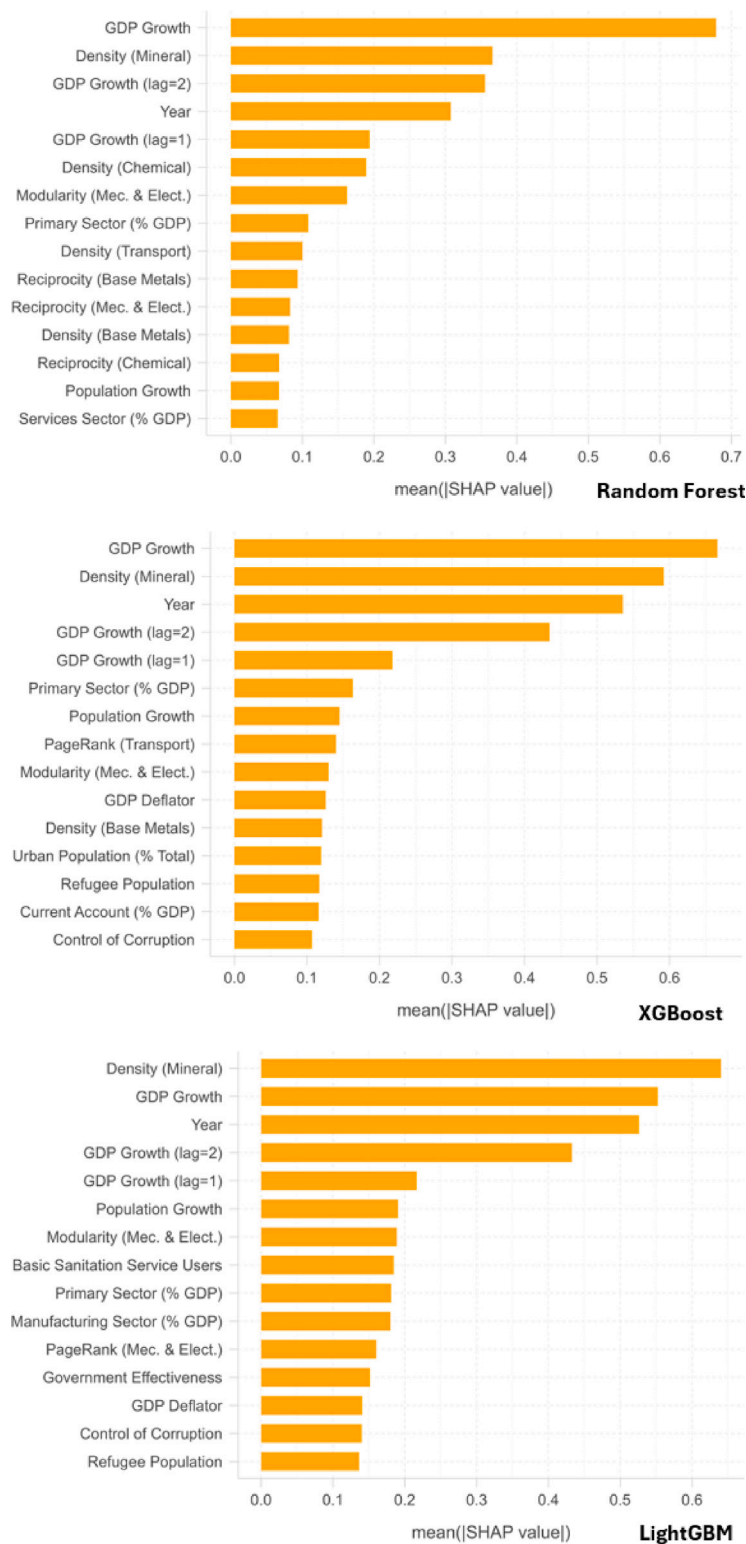


Fig. 3. This figure shows the average SHAP values for the Top 15 features based on predictive power across XGBoost, LightGBM, and Random Forest models.



feature. The density of the Mineral trade network is the second most critical feature for the Random Forest and XGBoost models, surpassing current GDP growth in the LightGBM model. Temporal dynamics rank as the third most significant feature for both the XGBoost and LightGBM models and fourth for the Random Forest model. The two-period lagged GDP growth rate secures the fourth position in the XGBoost and LightGBM models while it climbs to the third spot in the Random Forest model.

This initial analysis yields several insightful observations. Primarily, these four variables collectively form a core group that exhibits considerably large SHAP values relative to other features, highlighting their pivotal role in forecasting economic growth. Secondly, the significant positioning of both current and two-period lagged GDP growth rates suggests an “economic inertia” effect, indicating that present and recent economic performances have implications for future growth trajectories. Thirdly, the connectivity of trade networks plays a critical role in economic growth predictions, with particular emphasis on the Mineral section.

A notable discovery is the substantial representation of network metrics among the Top 15 features within the Random Forest model, the most effective model of our work. Remarkably, more than half of these leading features pertain to network metrics, with eight out of fifteen. Specifically, the metrics of density and reciprocity are especially prominent, constituting seven out of these eight network metrics. Furthermore, we observe that each of the five commodity sections covered in our study features at least one network metric among the top-ranking features, suggesting their overall significance in economic growth forecasts. This prevalence starkly contrasts with the findings from the other two models, where network metrics are considerably less represented, making up only three out of the Top 15 features.

Moreover, our research consistently highlights the importance of three variables across all three models: the modularity of the Mechanical & Electrical trade network, population growth, and the value added by agriculture, forestry, and fishing to GDP. This consistency across varied models underscores the significance of network connectivity, population dynamics, and the contributions of primary sector activities to predicting economic growth.

### 3.2.3. In-depth analysis of the Random Forest model

Our analysis shows that the Random Forest model is superior in predictive accuracy. Consequently, we select this model for an in-depth examination with regard to feature interpretability using Shapley values. We develop in Fig. 4 a beeswarm dependence plot to illustrate the Top 20 features, identified by the highest mean absolute SHAP values. The vertical axis of the plot orders the features by their significance in the model, while the horizontal axis displays standardized SHAP values. Each dot in the plot symbolizes the marginal contribution of a specific attribute for an individual observation, enabling the examination of SHAP value distributions through denser (indicating a higher concentration of observations) and sparser areas (indicating a lower concentration). Positive SHAP values indicate a positive contribution (increases) to the GDP growth in the following year. In contrast, negative values indicate a negative contribution (decreases) of the feature to the GDP growth in the following year. The coloration of dots indicates the attribute’s value: lighter (darker) colors represent higher (lower) values for the attribute.

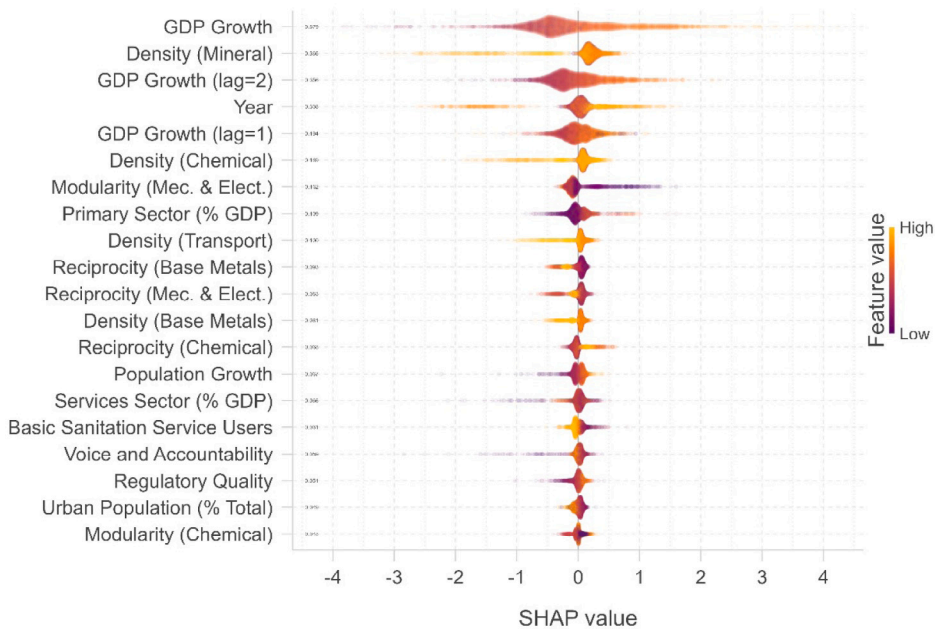


**Fig. 4.** This figure displays a beeswarm plot of the Top 20 features from the Random Forest model, ranked by their mean SHAP values. Features are ordered vertically by importance, with their standardized SHAP values plotted horizontally, showing the contribution to prediction. Dots represent individual observations, with their distribution indicating the variability of SHAP values; dense areas suggest higher concentration, while sparse areas indicate less. The color of the dots reflects the feature values, elucidating the influence of high versus low feature values on economic growth forecasts, with positive SHAP values signaling potential growth and negative values indicating possible downturns.

Our scrutiny begins with the most relevant feature: the current GDP growth. Observations with lower values of this feature have negative SHAP values, while higher values align with positive ones. This suggests that reduced current GDP growth rates portend a lower GDP growth next year and vice versa. This pattern is consistent with examining the two-period lagged GDP growth, reinforcing the “economic inertia” concept. This concurs with economic literature, which posits that economic growth exhibits an “autoregressive component”. This rationalizes the widespread use in the literature of autoregressive models as a baseline for comparison with more complex models [44].

The density of the Mineral trade network is the second most relevant attribute. The variability in this feature’s values is relatively low, as indicated by the dot coloration. Medium values are associated with positive SHAP values. In contrast, higher values correspond to negative SHAP values, suggesting an intriguing pattern: moderate to high network density values correlate with positive future economic growth, yet exceedingly high values forecast negative economic outcomes, implying a threshold beyond which network density inversely affects economic growth in the following year. This link between the Mineral trade network’s metric and future economic performance may be attributed to the influence of commodity prices — such as iron ore, oil, and coal — on business cycles [45]. Similar patterns are observed for the density measures of Chemical, Transport, and Base Metals trade networks.

A significant discovery relates to the feature associated with the primary sector. High values of this feature have positive SHAP values, while lower values align with negative SHAP values, indicating that an enhanced relevance of the primary sector within an economy forecasts positive economic growth in the following year and vice versa. This aligns with literature stating the crucial role of agriculture in shaping aggregate business cycles across countries [46].<sup>19</sup> Additionally, the patterns associated with population growth are noteworthy. Higher population growth values align with positive Shapley values, whereas lower values predict negative economic growth in the following year. This outcome aligns intuitively with conventional models of economic growth that posit the relevant role of population dynamics in driving economic performance [47].

We conclude our analysis by presenting in Fig. 5 the SHAP value dependence plots for five selected features of the Random Forest model. These plots augment the insights gained from the beeswarm dependence plot analysis by offering a nuanced view of how variations in feature values influence economic growth forecasts. On the horizontal axis, feature values are standardized, providing a vivid visual representation of how deviations from the average feature value — both positive and negative — affect predictions.

Commencing with the plot for current GDP growth, we observe that an increase of 1 standard deviation from the average current GDP growth induces a significant uptick in SHAP value. Further increments of a similar magnitude yield only marginally higher SHAP value, indicating a trend of diminishing marginal contributions to GDP growth in the following year. In contrast, a decrease of 1 standard deviation from the mean value leads to a decline in SHAP value, venturing into negative territory. Notably, SHAP values demonstrate lesser sensitivity to decreases of 1 standard deviation than to increases of the same magnitude relative to the mean value. Moreover, our analysis reveals a predominantly linear decline in SHAP values as decreases extend to 3 standard deviations below the mean.

Shifting the focus to the network density of the Mineral trade network, we identify patterns distinctly different from those associated with current GDP growth. Variations in network density ranging from  $-2$  to about  $-0.8$  standard deviations from the average feature value exert no influence on SHAP values. However, within the span of  $-0.8$  to approximately  $0.3$  standard deviations from the mean, SHAP values trend positively. Elevating network density beyond  $0.3$  standard deviations from the mean triggers a marked negative trajectory, with SHAP values descending into increasingly negative realms. This pattern underscores a complex relationship: while moderate increases in network density within the mineral section are correlated with neutral or positive effects on economic growth in the following year, surpassing a critical threshold links further increases in network density with declining future economic prospects, suggesting an optimal range for network density enhancements to positively influence future economic growth.

Subsequently, we delve into an additional network metric: reciprocity of the Base Metals section. Our analysis delineates three distinct intervals, each characterized by varying behaviors of SHAP values in response to changes in reciprocity. In the interval between  $-1$  and  $-0.3$  standard deviations, the SHAP values manifest a positive trend, where increments in reciprocity correlate with higher SHAP values. Conversely, in the range from  $-0.3$  to  $2$  standard deviations, an increase in reciprocity decreases SHAP values, which ultimately become negative. Finally, within the interval spanning from  $-2$  to  $-2.5$  standard deviations, although increases in reciprocity are associated with elevated SHAP values, these adjustments are insufficient to revert them to positive figures. This observation underscores a notable result: reciprocity values below the average are associated with positive GDP growth in the subsequent year, whereas reciprocity levels above the average indicate negative GDP growth forecasts.

In our evaluation of the value added by agriculture, forestry, and fishing activities to GDP, positive deviations within the range of  $0$  to  $1$  standard deviation from the mean yield positive and ascending SHAP values. Between  $1$  to  $2$  standard deviations, SHAP values level off, signifying a stabilization in their predictive impact. Beyond two standard deviations, we observe a gradual descent in SHAP values. Conversely, intervals between  $-1$  and  $0$  standard deviations from the mean feature value show negative SHAP values, following an approximately linear decline. These observations suggest that positive deviations from the mean can enhance

<sup>19</sup> Economies heavily reliant on agriculture experience pronounced fluctuations in overall output, exhibit low relative volatility in aggregate employment, and demonstrate a weak correlation between output and employment. Moreover, agriculture is distinctively characterized by more volatile output and employment, which are not positively correlated with those in other sectors. There is a weaker correlation between output and employment within agriculture than in non-agricultural sectors. These unique characteristics significantly influence the dynamics of aggregate business cycles across countries [46].

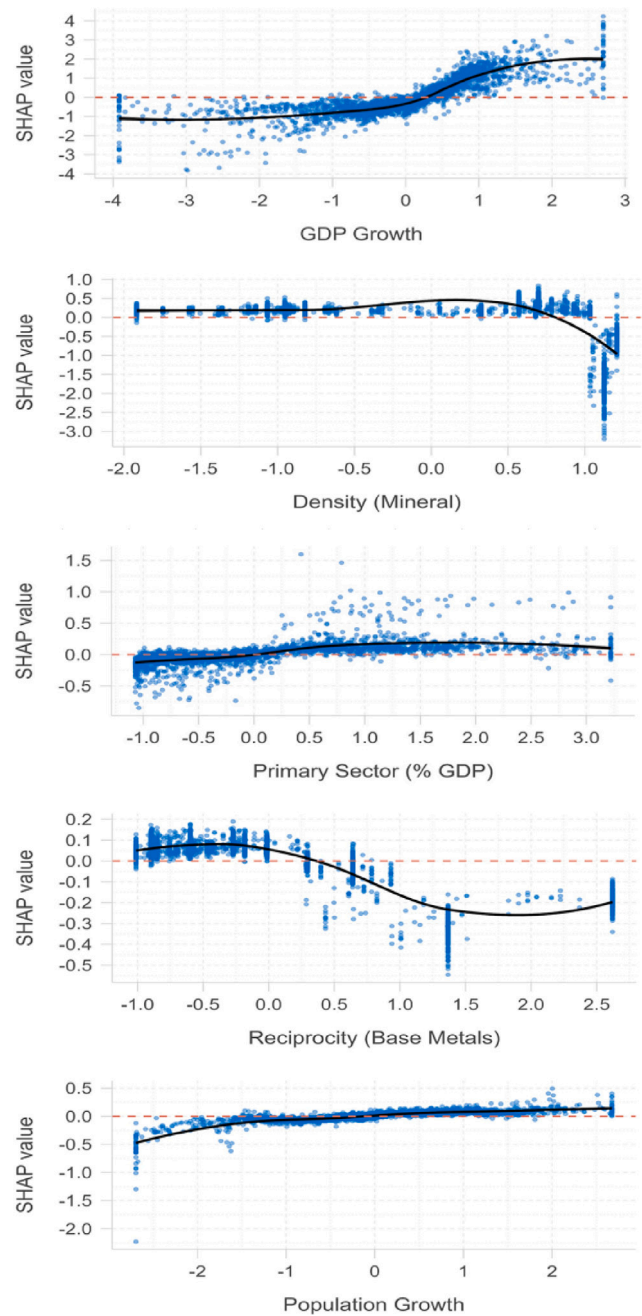


**Fig. 5.** This figure showcases the SHAP value dependence plots for five key features of the Random Forest model. These plots elucidate the nuanced relationships between variations in feature values and their impact on predictive outcomes. By standardizing feature values along the horizontal axis, the plots effectively demonstrate how both positive and negative deviations from the mean feature value contribute to changes in the model's economic growth predictions.

economic growth forecasts (up to two standard deviations), while negative deviations are associated with diminished economic prospects.

Lastly, we analyze population growth, identifying a linear relationship in SHAP values within the range of  $-1.5$  to  $2$  standard deviations from the mean feature value. Values below the mean correlate with negative SHAP values, and those above the mean with positive SHAP values. We note an accelerated decline in SHAP value for feature values descending beyond  $-1.5$  standard deviations from the mean. This indicates that within the predominant range of feature values, the relationship between population growth and economic growth in the following year is approximately linear, except at significant negative deviations from the mean, where the impact on economic growth forecasts intensifies.

#### 4. Conclusions

We reflect on our efforts to elucidate the intricate relationship between international trade networks and machine learning techniques in forecasting economic growth. Our objective was to go beyond traditional forecasting methodologies by harnessing the predictive power of network topological measures alongside advanced machine learning models. Central to our findings is the recognition of the necessity for models that can unravel complex patterns and non-linear relationships while integrating international trade networks as pivotal features to refine economic growth forecasts.

Our detailed analysis began with constructing section-level international trade networks and extracting topological measures, which unveiled significant transformations within these networks amid de-globalization trends. The pivotal period identified between 2016 and 2018, marked by a reversal of prior trends, highlighted the deep-seated impact of trade policy uncertainties intensified by global events such as the USA–China trade war, the COVID-19 pandemic, and Russia's invasion of Ukraine. The centrality rankings we developed revealed shifting paradigms of influence within the international trade domain, emphasizing the sustained dominance of certain nations and the notable rise of others, like India, in key commodity-specific trade networks.

Moreover, our venture into machine learning for economic growth forecasting revealed the superior performance of models such as Random Forest, XGBoost, and k-NN over traditional linear regression models. This finding confirms the complex and non-linear patterns these advanced models capture and highlights the critical role of network measures in boosting forecasts' accuracy. In particular, the density of the Mineral trade network stood out as a pivotal predictor, showcasing the nuanced interplay between trade network dynamics and economic forecasting.

Our feature importance analysis highlighted the autoregressive nature of economic growth, underscoring the imperative of grasping both past and present GDP dynamics to predict future economic performance effectively. This insight is further enriched by identifying key growth predictors, such as the modularity of the Machine & Electrical trade network, population growth, and the significance of the primary sector. The consistent importance of these factors across the top-performing models underscores their essential role in predicting future economic performance.

Delving into feature interpretability, particularly through the Random Forest model, we uncovered the complex ways key features influence economic forecasts. The use of SHAP value dependence plots proved crucial in deciphering these patterns, for instance, demonstrating how variations in the Mineral trade network's density correlate with GDP growth predictions. Identifying an optimal network density range highlights the need for nuanced policies and decision-making to leverage network topological analysis benefits while mitigating potential drawbacks.

Looking to the future, there is ample scope for expand this research. Delving deeper into the causal links between network topologies and economic outcomes, incorporating real-time data, and exploring predictive models in light of sudden economic shocks or geopolitical developments could offer critical insights for policymakers striving for resilience and adaptability in an ever-changing and dynamic global landscape.

#### Ethical statement

The authors have no conflicts of interest to declare that are relevant to the content of this article.

#### CRediT authorship contribution statement

**Thiago Christiano Silva:** Writing – review & editing, Writing – original draft, Supervision, Software, Methodology, Investigation, Funding acquisition, Data curation, Conceptualization. **Paulo Victor Berri Wilhelm:** Writing – review & editing, Writing – original draft, Validation, Software, Resources, Methodology, Investigation, Formal analysis, Data curation. **Diego R. Amancio:** Writing – review & editing, Software, Investigation, Formal analysis.

#### Declaration of competing interest

The authors declare that they have no known competing financial interests or personal relationships that could have appeared to influence the work reported in this paper.

#### Data availability

Data will be made available on request.

#### Acknowledgments

Thiago C. Silva (Grant no. 302703/2022-5) and Diego R. Amancio (Grant no. 311074/2021-9) gratefully acknowledge financial support from the CNPq foundation. Diego R. Amancio also acknowledges financial support from FAPESP (Grant no. 20/06271-0). Paulo V. B. Wilhelm gratefully acknowledges financial support from the CAPES foundation.

## Appendix A. Complex network measures

In this section, we define the complex network measures used in our work and specify the graph representations required for each measure. The network metrics are calculated using RStudio (version 2023.09.0 Build 463) and R (version 4.3.1), employing the igraph package (version 1.5.1).

- *Strength (strictly local)*: defined by the aggregate weight of edges connected to a node, node strength in directed graphs splits into in-strength and out-strength. In-strength calculates the total weight of incoming edges to a node, analogous to a country's total import value within a specific trade section. Conversely, out-strength tallies the weight of outgoing edges, akin to a country's total export value.
- *PageRank (mixed)*: by leveraging the classic PageRank coefficient, we determine the relative importance or centrality of countries within the trade network. A country's centrality reflects not just its direct trade connections but also the significance of its trading partners. PageRank emphasizes incoming edges, which, within the framework of our analysis, are interpreted as import flows. Consequently, this centrality measure recognizes a country's influence within the network based on its import performance. Additionally, we consider a variation of PageRank that emphasizes outgoing edges, which represent export flows, thus highlighting a country's influence based on its export performance.
- *Clustering coefficient or Transitivity (mixed)*: this metric evaluates the degree to which nodes in the network cluster together, calculated by the ratio of actual triangles to potential triangles among nodes. An actual triangle is a set of three nodes that are all directly connected to each other, forming a closed loop. A potential triangle is a set of three nodes where at least two nodes are directly connected, creating the possibility of forming a triangle if the third connection exists. High clustering coefficients (close to 1) indicate a high level of local clustering, while low values (close to 0) suggest a more dispersed trade network.
- *Density (global)*: provides a snapshot of the fulfillment of the network's connectivity potential, measured by the ratio of actual to possible connections. A higher proportion of potential trade links are realized in dense trade networks, indicating a closely interconnected global trade fabric.
- *Assortativity (global)*: evaluates the degree to which edges in the network join nodes sharing analogous attributes. We employ the assortativity degree coefficient, which measures the frequency of connections between nodes with similar degrees. A value close to 1 indicates an assortative network, suggesting that many trade connections occur between countries with similar numbers of trading partners, whether they are many or few. On the other hand, a value close to  $-1$  points to a disassortative network. This reflects a pattern where trade connections frequently exist between countries with disparate numbers of trading partners—one with a high number of partners and the other with a low number. This approach clarifies the nature of connectivity within the international trade network, revealing the tendencies for countries to trade with partners of similar or dissimilar connectivity levels.
- *Reciprocity (global)*: calculates the extent of mutual exchanges within the network based on the proportion of reciprocated connections relative to the total number of connections. A high reciprocity level, approaching 1, indicates that most trade partnerships involve mutual exchanges. Conversely, a low reciprocity level, nearing 0, suggests that the bulk of trade flows occurs in one direction between trade partners.
- *Modularity (global)*: explores how the network is segmented into distinct communities or modules, characterized by dense connections within each community and fewer connections between different communities. High modularity values, approaching 1, signal that connections within communities significantly outnumber those between communities. Conversely, values near 0 indicate a balance between connections within communities and those bridging different communities. This evaluation highlights the network's structure, identifying whether it is more segregated into tightly-knit groups or integrated, with fluid interactions across different groups. The modularity is calculated based on the membership of nodes as determined by the Walktrap community detection algorithm, with a resolution parameter of 1, considering the directed nature of the graph.

We employ two directed graph representations: one weighted and the other unweighted (see [Table A.1](#)).

**Table A.1**

Graph representations and network metrics.

Metric	Graph representation			
	Directed	Undirected	Weighted	Unweighted
Density	X			X
Assortativity	X			X
Reciprocity	X			X
Transitivity	X			X
Modularity	X		X	
Strength	X		X	
PageRank	X		X	

**Notes:** The table summarizes the types of graph representations applicable for each network metric.



## Appendix B. Machine learning methods

This section reviews the suite of supervised regressions that constitute the horse race of algorithms. We represent vectors using bold lowercase.

- Linear Regression

Linear Regression is a foundational statistical method employed for modeling the relationship between a dependent variable and one or more independent variables by optimizing the parameters of a linear equation to best fit the observed data [48,49]. The core principle of Linear Regression lies in minimizing the sum of the squared differences between the observed outcomes in the dataset and the outcomes predicted by the linear approximation. Mathematically, this optimization problem can be expressed as minimizing the cost function  $J(\theta) = \frac{1}{2m} \sum_{i=1}^m (h_{\theta}(\mathbf{x}^{(i)}) - y^{(i)})^2$ , where  $m$  denotes the number of observations,  $h_{\theta}(\mathbf{x})$  represents the hypothesis function defined by  $h_{\theta}(\mathbf{x}) = \theta^T \mathbf{x}$ ,  $\theta$  are the parameters to be optimized,  $\mathbf{x}^{(i)}$  denotes the vector of independent variables (features) for the  $i$ th observation and  $y^{(i)}$  represents the actual observed value for the  $i$ th observation. The algorithm selects  $\theta$  such that it minimizes the cost function  $J$  discussed above. Since  $J$  is convex, the optimization process admits a closed-form solution, often called the ordinary least squares method. Linear regression has no hyperparameters.

- Elastic Net (Linear Regression with regularization)

Regularized variants of Linear Regression, such as Ridge Regression (L2 regularization) and Lasso Regression (L1 regularization), introduce a penalty term to the cost function in the linear regression to prevent overfitting by constraining the magnitude of the model coefficients. Elastic Net Regression combines the strengths of both L1 and L2 regularization methods [50]. This approach is particularly effective in scenarios where multiple features are correlated and aims to balance the complexity of the model with its performance, thereby mitigating the issue of model overfitting. The cost function for Elastic Net Regression is formulated by incorporating both L1 and L2 penalty terms, optimizing the equation  $J(\theta) = \frac{1}{2m} \sum_{i=1}^m (h_{\theta}(\mathbf{x}^{(i)}) - y^{(i)})^2 + \lambda_1 \sum_{j=1}^n |\theta_j| + \lambda_2 \sum_{j=1}^n \theta_j^2$ , where  $\lambda_1$  and  $\lambda_2$  are the regularization parameters for the L1 and L2 penalties, respectively. This dual regularization approach allows Elastic Net to inherit the feature selection property of Lasso while also retaining the regularization benefits of Ridge, making it a versatile tool for regression analysis involving high-dimensional datasets. The hyperparameters we tune in the model selection are both  $\lambda_1$  and  $\lambda_2$ .

- Support Vector Machine

Support Vector Machine (SVM) with Radial Basis Function (RBF) kernel is a non-linear method [51]. Unlike Linear Regression, which minimizes the discrepancies between observed and predicted values within a linear context, SVM with RBF kernel models complex, non-linear relationships in regression tasks. The SVM algorithm seeks to find the optimal hyperplane in a high-dimensional space that maximizes the margin (distance) of the hyperplane to the nearest points of each class, called support vectors. The RBF kernel is instrumental in transforming the input data into a higher-dimensional space, where linear regression becomes possible, thereby effectively handling non-linear data structures. The optimization function critical to SVM with RBF kernel for regression is formulated as minimizing  $J(\theta) = \frac{1}{2} \|\theta\|^2 + C \sum_{i=1}^m (\max(0, |y^{(i)} - (\theta^T \phi(\mathbf{x}^{(i)}) + b)| - \epsilon))^2$ , where  $C$  is the regularization parameter,  $\phi(\mathbf{x}^{(i)})$  represents the high-dimensional space mapped by the RBF kernel,  $b$  is the bias, and  $\epsilon$  denotes a margin of tolerance within which no penalty is given to errors. The parameter  $\gamma$  in the RBF kernel function, defined as  $\gamma = \frac{1}{2\sigma^2}$ , plays a critical role in determining the decision boundary's flexibility. This optimization ensures that the model balances the complexity and the fitting accuracy, making SVM with RBF kernel a powerful tool for tackling non-linear regression challenges. The hyperparameters we tune in the model selection are  $C$  and  $\gamma$ .

- k-Nearest Neighbor

The k-Nearest Neighbor (k-NN) algorithm stands out in the machine learning landscape for its simplicity and non-parametric nature, contrasting sharply with the complexity of SVM with RBF kernel and the linearity of Linear Regression [52]. k-NN operates on the principle of feature similarity, predicting the outcome for a new instance based on the majority vote or average of its  $k$  closest neighbors in the feature space. This straightforward approach eliminates the need for parameter estimation, presenting an advantage in terms of simplicity and interpretability. Additionally, the performance heavily depends on the choice of  $k$  and the distance metric, which can significantly affect its accuracy. Unlike previous models, k-NN does not optimize a specific function for learning; instead, it directly uses the training data for prediction, minimizing an implicit cost function related to the distance between the query instance and its nearest neighbors, thereby determining the best fit for prediction. Despite its simplicity, k-NN's effectiveness is contingent upon a careful balance between the choice of  $k$  and the distance metric, ensuring adequate performance while highlighting its intuitive approach to machine learning prediction outcomes. The hyperparameter we tune in the model selection is  $k$ .

- Random Forest

The Random Forest algorithm is a prominent ensemble learning method designed to refine regression analyses through the collective predictions of multiple decision trees [53]. This ensemble technique aims to elevate the robustness and accuracy of the model by merging the outputs from a variety of base learners, effectively mitigating the risk of overfitting common in more complex models. Specifically, Random Forest improves model generalization by averaging the individual predictions ( $\hat{y}_n$ ) from each of the  $N$  decision trees, making the ensemble's final prediction more reliable across diverse datasets. For a Random Forest composed of  $N$  trees, the prediction  $\hat{y}$  for any given input is calculated by averaging the outputs of all trees, represented as  $\hat{y} = \frac{1}{N} \sum_{n=1}^N \hat{y}_n$ . The hyperparameters that we tune in the model selection are the number of trees ( $N$ ), the maximum depth of each tree ( $D$ ), and the number of features considered for splitting at each node ( $F$ ).

- **XGBoost**

XGBoost, an abbreviation for eXtreme Gradient Boosting, represents a sophisticated evolution of gradient boosting frameworks, acclaimed for its efficiency, versatility, and proficiency in processing large datasets [54]. Unlike Random Forest, which generates independent trees in a parallel fashion, XGBoost constructs each tree sequentially. XGBoost distinguishes itself by adeptly managing linear and nonlinear datasets and incorporating regularization directly into its optimization process to mitigate overfitting. This regularization introduces penalties on the model's complexity, thereby balancing the reduction of prediction errors with the control of model complexity. The objective function optimized by XGBoost in regression tasks incorporates a regularized component, defined as  $J(\theta) = \sum_{i=1}^m l(y^{(i)}, \hat{y}^{(i)}) + \sum_k \Omega(f_k)$ , where  $l$  signifies the loss function that measures the discrepancy between actual values  $y^{(i)}$  and predictions  $\hat{y}^{(i)}$ , and  $\Omega$  denotes the regularization term affecting the complexity of the model's trees. The hyperparameters that we tune in the model selection are the learning rate ( $\eta$ ), the maximum depth of the trees ( $D$ ) and the regularization parameters ( $\lambda$  for L2 regularization,  $\alpha$  for L1 regularization).

- **Light Gradient Boosting Machine**

Light Gradient Boosting Machine (LightGBM), an advanced gradient boosting framework, excels in predictive modeling by optimizing a loss function  $L = \sum_{i=1}^m l(y_i, \hat{y}_i)$ , methodically incorporating weak learners in successive iterations through the formula  $F_{k+1}(x) = F_k(x) + \alpha \cdot h(x)$  [55]. It sets itself apart with unique features like Gradient-based One-Side Sampling (GOSS)<sup>20</sup> and Exclusive Feature Bundling (EFB),<sup>21</sup> which substantially boost its computational efficiency. Directly comparing LightGBM to its counterpart, XGBoost, reveals LightGBM's advantage in terms of reduced memory usage and faster execution times thanks to these innovations while maintaining comparable levels of predictive accuracy. The approach to building trees sets LightGBM apart from XGBoost and other prevalent algorithms. Where many algorithms expand trees in a sequential, level-wise manner, LightGBM adopts a strategy focused on expanding trees by leaves, specifically targeting the leaf that is anticipated to result in the largest decrease in loss. In addition, while XGBoost and numerous other algorithms utilize a sorted-based method for learning decision trees — seeking the best division points among ordered attribute values — LightGBM employs a unique, histogram-based method. This model captures complex, non-linear relationships without requiring extensive feature engineering. This capability is fine-tuned through the adjustment of key hyperparameters such as the number of leaves ( $L$ ), learning rate ( $\eta$ ), and maximum depth of trees ( $D$ ). These parameters play a crucial role in the model's performance, as encapsulated in the equation  $F_{k+1}(x) = F_k(x) + \eta \cdot h_k(x, L, D)$ , highlighting the sensitivity of LightGBM's output to these hyperparameters.

Understanding the computation time for predictions at test time for different machine learning techniques in terms of Big O notation is essential for evaluating their efficiency and suitability for various applications. Here's an analysis for each of the mentioned techniques:

- **Support Vector Machine (SVM)**

**Big O Notation:**  $O(n \cdot D)$

*Explanation:* The prediction time complexity of a Support Vector Machine (SVM) depends on the number of support vectors and the dimensionality of the feature space. The number of support vectors can be as large as the size of the training set, denoted by  $n$ . Each prediction requires computing the distance to each support vector, and this distance computation is influenced by the dimensionality of the feature space,  $D$ . Therefore, the overall prediction time complexity is  $O(n \cdot D)$ .

- **Light Gradient Boosting Machine (LightGBM)**

**Big O Notation:**  $O(m \cdot \log(n))$

*Explanation:* LightGBM uses histogram-based algorithms and leaf-wise tree growth. The prediction time primarily depends on the depth of the trees, which is typically logarithmic in relation to the number of data points,  $n$ . The total prediction time is also affected by the number of trees,  $m$ . Therefore, the complexity is  $O(m \cdot \log(n))$ .

- **k-Nearest Neighbor (k-NN)**

**Big O Notation:**  $O(n \cdot D)$

*Explanation:* For k-NN, predicting a new instance requires comparing it to every instance in the training set, leading to a complexity of  $O(n \cdot D)$ , where  $D$  is the dimensionality of the feature space.

- **Random Forest**

**Big O Notation:**  $O(m \cdot \log(n))$

*Explanation:* Random Forest involves predicting with multiple decision trees. Each tree prediction involves traversing from root to leaf, which is logarithmic in the number of data points,  $n$ . The total time is multiplied by the number of trees,  $m$ .

- **XGBoost**

**Big O Notation:**  $O(m \cdot \log(n))$

*Explanation:* Similar to Random Forest, XGBoost is an ensemble of trees. Each tree's prediction involves a logarithmic traversal based on the tree depth. The overall complexity is a product of the number of trees,  $m$ , and the logarithmic traversal time.

<sup>20</sup> GOSS (Gradient-based One-Side Sampling) gives preference to instances with larger gradients, indicating that they are more difficult to predict accurately, thereby focusing the learning process on these harder examples.

<sup>21</sup> EFB (Exclusive Feature Bundling) aggregates sparse features that are mutually exclusive, reducing the dimensionality of the dataset with minimal loss of information.

- **Elastic Net**

**Big O Notation:**  $O(D)$

**Explanation:** Elastic Net is a linear model combining L1 and L2 regularization. The prediction time is linear with respect to the number of features,  $D$ , since it involves computing a weighted sum of the features.

- **Linear Regression**

**Big O Notation:**  $O(D)$

**Explanation:** Linear Regression prediction time is also linear with respect to the number of features,  $D$ , as it involves computing the dot product between the feature vector and the model coefficients.

## References

- [1] G. Elliott, A. Timmermann, Economic forecasting, *J. Econ. Lit.* 46 (1) (2008) 3–56.
- [2] J.G. De Gooijer, R.J. Hyndman, 25 Years of time series forecasting, *Int. J. Forecast.* 22 (3) (2006) 443–473.
- [3] R.P. Masini, M.C. Medeiros, E.F. Mendes, Machine learning advances for time series forecasting, *J. Econ. Surv.* 37 (1) (2023) 76–111.
- [4] T.C. Silva, P.V.B. Wilhelm, B.M. Tabak, The effect of interconnectivity on stock returns during the global financial crisis, *North Amer. J. Econom. Finance* 67 (2023) 101940.
- [5] K.T. Chi, J. Liu, F.C. Lau, A network perspective of the stock market, *J. Empir. Financ.* 17 (4) (2010) 659–667.
- [6] A. Samitas, E. Kampouris, S. Polyzos, COVID-19 pandemic and spillover effects in stock markets: A financial network approach, *Int. Rev. Financ. Anal.* 80 (2022) 102005.
- [7] T.C. Silva, S.M. Guerra, M.A. da Silva, B.M. Tabak, Micro-level transmission of monetary policy shocks: The trading book channel, *J. Econ. Behav. Organ.* 179 (2020) 279–298.
- [8] T.K. Lee, J.H. Cho, D.S. Kwon, S.Y. Sohn, Global stock market investment strategies based on financial network indicators using machine learning techniques, *Expert Syst. Appl.* 117 (2019) 228–242.
- [9] M. Demirel, F.X. Diebold, L. Liu, K. Yilmaz, Estimating global bank network connectedness, *J. Appl. Econometrics* 33 (1) (2018) 1–15.
- [10] T. Chuluun, A. Prevost, A. Upadhyay, Firm network structure and innovation, *J. Corp. Finance* 44 (2017) 193–214.
- [11] T.C. Silva, S.R.S. Souza, B.M. Tabak, Monitoring vulnerability and impact diffusion in financial networks, *J. Econom. Dynam. Control* 76 (2017) 109–135.
- [12] D. Garlaschelli, M.I. Loffredo, Fitness-dependent topological properties of the world trade web, *Phys. Rev. Lett.* 93 (18) (2004) 188701.
- [13] M. Barthélemy, A. Barrat, R. Pastor-Satorras, A. Vespignani, Characterization and modeling of weighted networks, *Physica A* 346 (1–2) (2005) 34–43.
- [14] C. Gao, M. Sun, B. Shen, Features and evolution of international fossil energy trade relationships: A weighted multilayer network analysis, *Appl. Energy* 156 (2015) 542–554.
- [15] W. Zhong, H. An, L. Shen, W. Fang, X. Gao, D. Dong, The roles of countries in the international fossil fuel trade: An emergy and network analysis, *Energy Policy* 100 (2017) 365–376.
- [16] C. Wang, L. Zhao, M.K. Lim, W.-Q. Chen, J.W. Sutherland, Structure of the global plastic waste trade network and the impact of China's import Ban, *Resour. Conserv. Recycl.* 153 (2020) 104591.
- [17] S. Torreggiani, G. Mangioni, M.J. Puma, G. Fagiolo, Identifying the community structure of the food-trade international multi-network, *Environ. Res. Lett.* 13 (5) (2018) 054026.
- [18] X. Hu, C. Wang, M.K. Lim, W.-Q. Chen, Characteristics of the global copper raw materials and scrap trade systems and the policy impacts of China's import ban, *Ecol. Econom.* 172 (2020) 106626.
- [19] Y. Ma, M. Wang, X. Li, Analysis of the characteristics and stability of the global complex nickel ore trade network, *Resour. Policy* 79 (2022) 103089.
- [20] M. Lovrić, R. Da Re, E. Vidale, D. Pettenella, R. Mavsar, Social network analysis as a tool for the analysis of international trade of wood and non-wood forest products, *Forest Policy Econom.* 86 (2018) 45–66.
- [21] Q. Shi, X. Sun, M. Xu, M. Wang, The multiplex network structure of global cobalt industry chain, *Resour. Policy* 76 (2022) 102555.
- [22] T.C. Silva, P.V. Wilhelm, D.R. Amancio, Interconnectivity disrupted by fading globalization: A network approach to recent international trade developments, *J. Phys.: Complex.* 5 (2024) 025018.
- [23] D. Caldara, M. Iacoviello, P. Molligo, A. Prestipino, A. Raffo, The economic effects of trade policy uncertainty, *J. Monetary Econ.* 109 (2020) 38–59.
- [24] C. Chuku, A. Simpasa, J. Oduor, Intelligent forecasting of economic growth for developing economies, *Int. Econ.* 159 (2019) 74–93.
- [25] A. Richardson, T. van Florenstein Mulder, T. Vehbi, Nowcasting GDP using machine-learning algorithms: A real-time assessment, *Int. J. Forecast.* 37 (2) (2021) 941–948.
- [26] S.D. Vrontos, J. Galakis, I.D. Vrontos, Modeling and predicting US recessions using machine learning techniques, *Int. J. Forecast.* 37 (2) (2021) 647–671.
- [27] P. Goulet Coulombe, M. Leroux, D. Stevanovic, S. Surprenant, How is machine learning useful for macroeconomic forecasting? *J. Appl. Econometrics* 37 (5) (2022) 920–964.
- [28] H. Hegre, J.R. Oneal, B. Russett, Trade does promote peace: New simultaneous estimates of the reciprocal effects of trade and conflict, *J. Peace Res.* 47 (6) (2010) 763–774.
- [29] L. Anghinoni, L. Zhao, D. Ji, H. Pan, Time series trend detection and forecasting using complex network topology analysis, *Neural Netw.* 117 (2019) 295–306.
- [30] M.H. Pesaran, T. Schuermann, L.V. Smith, Forecasting economic and financial variables with global VARs, *Int. J. Forecast.* 25 (4) (2009) 642–675.
- [31] T.C. Silva, L. Zhao, Machine Learning in Complex Networks, Springer, 2016.
- [32] M. Huchet-Bourdon, C. Le Mouél, M. Vijil, The Relationship between trade openness and economic growth: Some new insights on the openness measurement issue, *World Econ.* 41 (1) (2018) 59–76.
- [33] J.L. Butkiewicz, H. Yanikkaya, Institutional quality and economic growth: Maintenance of the rule of law or democratic institutions, or both? *Econ. Model.* 23 (4) (2006) 648–661.
- [34] H.S. Esfahani, M.T. Ramirez, Institutions, infrastructure, and economic growth, *J. Dev. Econ.* 70 (2) (2003) 443–477.
- [35] N. Benos, S. Zotou, Education and economic growth: A meta-regression analysis, *World Dev.* 64 (2014) 669–689.
- [36] K. Gyimah-Brempong, M. Wilson, Health human capital and economic growth in sub-Saharan African and OECD countries, *Q. Rev. Econ. Finance* 44 (2) (2004) 296–320.
- [37] M. Kuhn, Futility analysis in the cross-validation of machine learning models, 2014, arXiv preprint arXiv:1405.6974.
- [38] S.M. Lundberg, S.-I. Lee, A unified approach to interpreting model predictions, *Adv. Neural Inf. Process. Syst.* 30 (2017).
- [39] L.S. Shapley, A value for  $n$ -person games, in: Contributions to the Theory of Games, 1953, pp. 307–317.
- [40] E. Štrumbelj, I. Kononenko, Explaining prediction models and individual predictions with feature contributions, *Knowl. Inf. Syst.* 41 (2014) 647–665.
- [41] M. Smith, F. Alvarez, Identifying mortality factors from machine learning using Shapley values—a case of COVID-19, *Expert Syst. Appl.* 176 (2021) 114832.
- [42] G. Lee, J. Kim, C. Lee, State-of-health estimation of li-ion batteries in the early phases of qualification tests: An interpretable machine learning approach, *Expert Syst. Appl.* 197 (2022) 116817.

- [43] P. Giudici, E. Raffinetti, Shapley-lorenz explainable artificial intelligence, *Expert Syst. Appl.* 167 (2021) 114104.
- [44] G. Camba-Mendez, G. Kapetanios, R.J. Smith, M.R. Weale, An automatic leading indicator of economic activity: forecasting GDP growth for European countries, *Econom. J.* 4 (1) (2001) S56–S90.
- [45] M.J. Crucini, M.A. Kose, C. Otrók, What are the driving forces of international business cycles? *Rev. Econ. Dyn.* 14 (1) (2011) 156–175.
- [46] J.M. Da-Rocha, D. Restuccia, The role of agriculture in aggregate business cycles, *Rev. Econ. Dyn.* 9 (3) (2006) 455–482.
- [47] G.S. Becker, E.L. Glaeser, K.M. Murphy, Population and economic growth, *Amer. Econ. Rev.* 89 (2) (1999) 145–149.
- [48] K. Pearson, LIII. On lines and planes of closest fit to systems of points in space, *Lond. Edinb. Dublin Philos. Mag. J. Sci.* 2 (11) (1901) 559–572.
- [49] G.U. Yule, On the theory of correlation, *J. R. Statist. Soc.* 60 (4) (1897) 812–854.
- [50] H. Zou, T. Hastie, Regularization and variable selection via the elastic net, *J. R. Stat. Soc. Ser. B Stat. Methodol.* 67 (2) (2005) 301–320.
- [51] C. Cortes, V. Vapnik, Support-vector networks, *Mach. Learn.* 20 (1995) 273–297.
- [52] T. Cover, P. Hart, Nearest neighbor pattern classification, *IEEE Trans. Inform. Theory* 13 (1) (1967) 21–27.
- [53] L. Breiman, Random forests, *Mach. Learn.* 45 (2001) 5–32.
- [54] T. Chen, C. Guestrin, Xgboost: A scalable tree boosting system, in: *22nd ACM SIGKDD International Conference on Knowledge Discovery and Data Mining*, 2016, pp. 785–794.
- [55] G. Ke, Q. Meng, T. Finley, T. Wang, W. Chen, W. Ma, Q. Ye, T.-Y. Liu, Lightgbm: A highly efficient gradient boosting decision tree, *Adv. Neural Inf. Process. Syst.* 30 (2017).